18 CT and MR Angiography of the Brain and Carotid Arteries

Cesur Samanci

18.1 CT Angiography of the Brain and Carotid Arteries

The brain CTA is from C1 to vertex and the neck CTA is from the aortic arch to C1. In stroke imaging, head and neck CTA is performed from aortic arch to vertex, including Willis. For reducing the volume of contrast material (CM) and to prevent venous opacification, CT scannings are caudocranial [1–5]. CTA is a must in acute cerebrovascular disease. It is important to demonstrate the patency of intracranial vascular structures and the stenosis in the carotid artery in transient ischemic attack or stroke patients. The stenosis-forming plaque in the carotid artery may be the source of emboli. Besides, CTA shows exactly which segment of the vessel is occluded in patients undergoing mechanical thrombectomy [6–8]. CTA is more preferred than MRA in acute cases because of its speed. Evaluation of CTA in the evaluation of carotid artery stenosis (more than 70%) has a high specificity and sensitivity [9–17]. Single section CTA is not widely used in patients with CAS (Fig. 18.1). This may be due to the use of more than 100 mL of CM and a slice thickness of more than 2 mm. MDCT has eliminated most of these limitations. In addition to the use of less dose of CA, it allows obtaining less than 1 mm slice thickness and high resolution (HR) images [18–20]. In addition, MDCTA can show carotid arteries from the aortic arch to Willis in <15 seconds (s), with 1 mm slice thickness, HR, and most importantly low-dose CA [19, 20]. As the technology progresses in radiology, it has become important to reduce the dose of the CA, along with the radiation dose, in such a way as not to affect the image quality. Another way to reduce the amount of contrast agent (CA) is to give saline bolus immediately after administration [21–25]. de Monyé et al. [18] compared different volumes of CM at 16 detector row computed tomographic CTA of the carotid arteries. Patients included in the study were divided into three groups: Group 1 80 mL CA, Group 2 80 mL CA followed by 40 mL saline, and Group 3 60 mL CA followed by 40 mL saline. The Hounsfield unit was measured from the ascending aorta and arteries from the aorta at 1-s intervals. The attenuation was measured more than the other groups in patients who received 40 mL of the saline bolus in 80 mL of contrast. In the group with 60 mL CA, attenuation was lower than the other groups. Kim and colleagues [26] developed a contrast dose protocol for CTA at 64 detector CT for the diagnosis of acute cerebrovascular disease. A 70 mL CA (iohexol, Omnipaque 350 mgI/mL) and 25 mL saline bolus were given at a rate of 5 mL/s for CTA. About 1 min after CTA, CE brain CT was performed. The purpose of this brain CT after CTA is to demonstrate incidental lesions, sub-

C. Samanci (✉)
Istanbul University Cerrahpaşa Medical Faculty
Radiology Department, Istanbul, Turkey

S. M. Erturk et al. (eds.), *Medical Imaging Contrast Agents: A Clinical Manual*,
https://doi.org/10.1007/978-3-030-79256-5_18

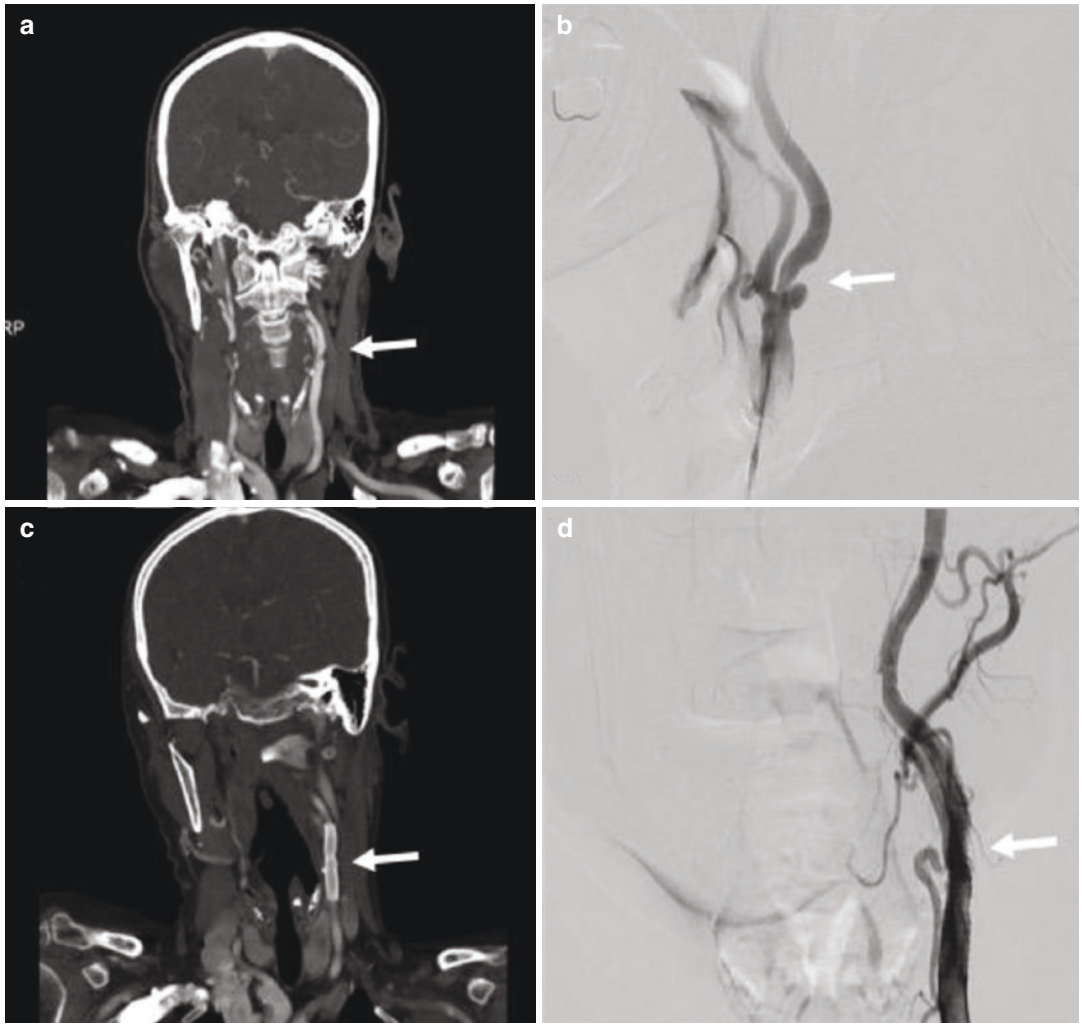

Fig. 18.1 CTA and digital subtraction angiography (DSA) of the carotid arteries before and after stenting. CTA MIP image (**a**) and DSA (**b**) of the left carotid artery stenosis before stenting. CTA MIP image (**c**) and DSA (**d**) of the left carotid artery after stenting

acute infarctions, hematoma, or contrast extravasation in aneurysm rupture. 150 mL of contrast medium (CM) is used (2 × 40 mL for CT perfusion and 70 mL for CTA). The total time of the procedure is approximately 8 min and the timing of contrast injection is very important for the best filling of the arteries. CA can be given with a delay of approximately 25 s. Since blood flow dynamics will change from patient to patient, it is useful to use the bolus tracking method especially in 64 section CT [26–29]. In a study by Kayan et al. [30], image resolution of carotid and cerebral CTA with a low voltage and low dose of CA was evaluated. Subjects were divided into two groups. CTA was performed with high-dose CA (1 mL/kg) and high-voltage (100 kv) in the first group and with low-dose CA (0.5 mL/kg) and low voltage (80 kv) in the second group. CA (iopromide, Ultravist 370, Bayer Schering Pharma, Berlin, Germany) with 370 mg iodine was used in both groups. The attenuation values were measured as HU from the lumen of the arteries and 300 HU and above were accepted as good image quality. The attenuation values

were over 300 in both groups. In other words, it is possible to perform carotid and cerebral CTA with low voltage and low CA with 128-detector CT. Thus, possible nephropathy and possible damaging effects of radiation are reduced. In another study about the reduction of the dose of CA, in one group cerebral CTA was performed with a moderate concentration of CA and 80 kV protocol, while the other group received a high concentration of CA with 120 kV [31]. Moderate concentration of CA with 80 kV protocol has better arterial opacification, has better signal to noise and contrast to noise ratios than a high concentration of CA with 120 kV protocol. Also, the iodine used in the low contrast group is about 18.9% less than the other group. Besides, subjective image quality is better, although less iodine is used. So giving less CA can reduce the risk of CIN, because it has less osmolality and less viscosity [31]. Similar to these studies, Nagayama et al. [32] demonstrate that under the 80 kVp (296 mgI/kg) with sinogram affirmed iterative reconstruction protocol, both the radiation and the CM dose were substantially reduced at cerebral bone subtraction CTA and that the image quality was better than on scans obtained with the standard 120 kVp (CA was 370 mgI/kg) with FBP protocol. In another study [33], the authors investigated results of low concentration CAs in craniocervical dual-energy CTA using a monoenergetic reconstruction method. In the first group, high concentration CA was used (iopromide 370) and in the second group low concentration CA was used (iopromide 270). Image qualities were comparable. So contrast dose could be reduced by the monoenergetic reconstruction method in craniocervical dual-energy CTA. Hinkmann et al. [34] evaluated the efficacy of low-dose contrast in carotid CTA using 128 slice ultra-fast (with a gantry rotation time of 300 ms) spiral CT. One group was studied with 80 mL contrast at a rate of 5 mL/s, while another group was studied with a 30 mL contrast, at a rate of 4 mL/s, followed by saline flushes in two groups. They used the test-bolus technique to calculate transit time in both groups. They showed that 30 mL of CM was sufficient to show arterial stenosis, vascular contrast density, and image quality.

In MDCTA volume of CA is related to the time of the procedure which is dependent on detector numbers [35].

50–100 mL CA containing about 350–370 mg iodine are used in carotid and cerebral CTAs depending on the patient size and speed of the scanner [36]. To achieve CTA attenuation of 250–350 HU for a 70 kg patient, 35 g iodine was administered at 1.4 g of iodine/s (100 mL of 350 mg of iodine/mL concentration at 4 mL/s) over 25 s is suggested for 16 detector CT, while 25 g of iodine injected at 1.6 g of iodine/s (75 mL of 350 mg of iodine/mL concentration at 4.5–5.0 mL/s) over 15 s is suggested for 64 detector CT, followed by a saline flush. When administration rates are decreased for a given CM volume to prolong the injection time for slower CT scanners, the magnitude of contrast enhancement will decline, if a higher iodine concentration CA is not given. Injection time appropriate to scan time may be estimated by using an approach, 15 s + (1/2) scan time. Speed of 4 mL/s is suggested for a 70 kg adult (slower injection for a smaller subject but faster for a larger subject), with a saline flush. In MDCT, a fixed delay time of 18–20 s is used for the cerebral CTA, 15 s for the carotid CTA [5]. Although the values are not certain, the duration of the injection is 15–20 s and the screening time can be 5–15 s. However, these values may not be appropriate even in an individual with normal circulation parameters. Therefore, it is important to use variable scan delays that allow variations to the patient while shooting. If it was assumed that the time to the peak contrast enhancement at the carotid artery is similar to the ascending aorta, the variable scan delay for carotid CTA may be determined as injection time + 5 − (1/2) scan time for an injection time more than 15 s or as 15 + (1/2) injection time − (1/2) scan time for an injection time 15 s or less (for a short injection, the CM transit time is governed more by intrinsic physiological circulation time of CM bolus than the injection time). Scan delay for cerebral CTA only is obtained by adding 3–5 s to carotid CTA. According to the patient's circulation, we use region of interest (ROI) to determine the scan delay. If we are going to perform carotid

and cerebral CTA, we put the ROI in ascending aorta, if we want to perform a cerebral only CTA, we place ROI over the aortic arch or mid carotid artery. When 12 s is used as the normal default value for CM arrival time in aortic arch, the time to peak aortic enhancement corresponds to injection time + (CM arrival time − 12) + (5 s) or injection time + CM arrival time − (7 s). So, at CM arrival time equals 12, the circulation adjusted and variable delay approaches become equivalent. CM arrival time would increase in subjects with slow circulation. From the equation, scan delay can be computed as injection time + CM arrival time − (7 s) − (1/2) scan time. For example, for a 10-s scan with a 20-s injection, scan delay would be 20 + CM arrival time − 7 − (10/2) or CM arrival time + 8. So, scan delay is determined by adding 8 s to CM arrival time measured from a test-bolus technique. On the other hand, when a bolus tracking technique is used, CM arrival time is not estimated prior to the injection of a full bolus of CM. CT scan will start at CM arrival time + 8, that is, 8 s of additional diagnostic delay after a time of reaching 50 HU enhancement threshold [36, 37]. A longer diagnostic delay will be required for a faster scan, a longer injection, and the brain-only CTA triggered at aorta but the scan started more distally at C1 level. MDCTA is a widely used method for brain imaging, especially in stroke (Fig. 18.2). However, in the 64-detector CT, the *z*-axis coverage is 3.2 cm and only allows for perfusion in small brain tissue around Willis and does not permit the evaluation of whole-brain circulation by dynamic angiography. Ruiz et al. [38] performed a whole head dynamic CTA using a 16 cm *z*-axis coverage with 320 detector MDCT in a patient with stenosis in the carotid. In addition to perfusion of the whole brain, all the vascular structures in the brain were demonstrated with dynamic subtracted angiography. CT with 320 detectors has uniquely increased *z*-axis coverage and is a very important innovation for all brain perfusion and subtracted dynamic angiography. It has a very important place in the first intention imaging of neurovascular diseases, especially in stroke [38].

When talking about CAs, it is even important that the CA is delivered from the right arm or the left arm. The purpose of the authors in a paper was to demonstrate the results of right and left-sided CA injection and mutual effects on the subject's age, gender, body weight, and arterial opacification in carotid and cerebral angiography. Their findings support preferential right-sided injection in subjects older than 40 years who have higher body mass index and weight in CTA procedures [39].

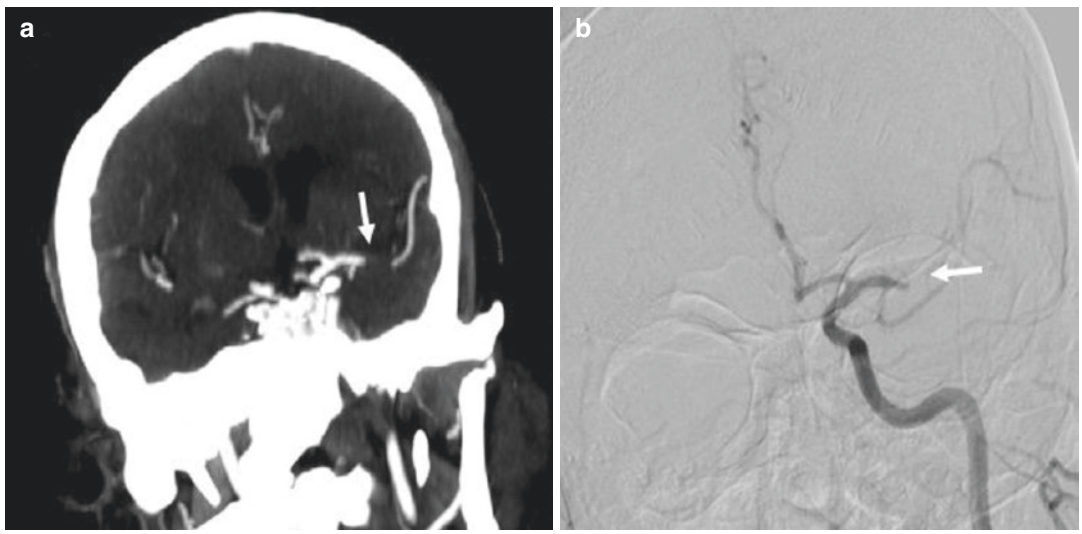

Fig. 18.2 CTA MIP image (**a**) and DSA (**b**) showing occlusion of left MCA M1segment

CE cone-beam CT plays an important role in stent imaging especially in patients with stent implantation due to intracranial aneurysm. Currently applied CE cone-beam CT images require a quantitative dilution of the CA to improve image quality. In a study, it was shown that this technique could be performed without quantitative contrast dilution. CM dilution for high image quality can be achieved from quantitative contrast infusion (0.2 cm^3/s) with saline flushes through a guiding catheter and using normal blood flow. Saline flush with a 300 mmHg pressure bag is suggested to show the relationship between stent strut and the parent artery and stent architecture [40].

Doerfler et al. [41] wanted to clarify whether iopromide, a nonionic CA, is safe in stroke. In their study rats underwent endovascular occlusion of the middle cerebral artery. Four hours later, they received iothalamate sodium and iopromide. Iopromide (Ultravist 370; Schering, Berlin, Germany) is available as a stable, clean, and colorless aqueous solution for parenteral injection; it has an iodine content of 370 mg/mL. The osmolality of the nonionic, monomeric solution was 770 mOsm per kilogram of water. Iothalamate sodium (Conray 70; Mallinckrodt, Hennef, Germany) is an ionic, iodinated CA that is available as an aqueous solution for parenteral injection; it has 420 mg/mL iodine. Lothalamate sodium contains sodium salt of iothalamic acid. The adequate dose is 588 mg of iodine per kilogram body weight. The osmolality of the solution was 2520 mOsm per kilogram of water. Bolus injection of the nonionic iopromide does not statistically significantly affect infarction volume or cerebral ischemia symptoms. The ionic CA iothalamate sodium caused higher mortality and morbidity and increased infarction volume in rats. Nonionic rather than ionic CAs should be preferred during acute cerebral ischemia.

While the carotid CTA is performed, the CA from the arm is not yet diluent, so it causes perivenous artifacts especially at the level of the subclavian vein, brachiocephalic vein, and superior vena cava [42, 43]. These artifacts cause a possible pathology to be missed in the main arteries originating from the aortic arch. In one study, the authors tested how these perivenous artifacts were affected by the craniocaudal scan direction and the caudocranial scan direction. In CTAs with 16-detector MDCT, low attenuation in the carotid artery and low attenuation in superior vena cava were obtained in the craniocaudal direction. Streak artifacts were significantly decreased and a better evaluation was obtained in the arteries originating from the arch [44].

Since the autopsy is highly traumatic for the family of the deceased person, it is particularly undesirable for the relatives of the deceased. Postmortem imaging may be a good alternative to autopsy and is now becoming increasingly popular. There is a lot of research on this subject, for example, Ross et al. [45] have tried to establish a contrast protocol for whole body CTA. They evaluated the results by comparing lipophilic and hydrophilic CAs. In the first group, paraffin oil and iodized oil (Lipiodol Ultra Fluide, Guerbet) were used in a ratio of 15/1. In the other group, the PEG solution (PEG 200, Schaerer-Schlaepfer AG) and iopentol (Imagopaque 300, GE-Healthcare) were perfused to be 10/1 (average density 600 HU). In these images, end portions of vascular structures and small extravasations were shown better than those in alive patients.

An inguinal incision was made before imaging and retrograde cannulation in femoral artery and antegrade cannulation in femoral vein was performed. 2000 mL was perfusion volume, 80 mmHg was perfusion pressure, 800 mL/min was flow rate for head and neck CTA. Postmortem angiography using PEG is successful in visualizing tissues showing good vascularization and prevents unintended gastrointestinal extravasation [45].

18.2 MR Angiography of the Brain and Carotid Arteries

CE MRI can show many pathologies that are not seen in non-CE imaging [46–52]. In 1988, Gd-DTPA (Magnevist), the first specific CA that is compatible with MRI, was released [53]. These MR-compatible CAs showed considerable variation over time. These extracellular, gadolinium-

based CAs show kidney excretion and are increasingly used in routine clinical practice over the years. Gadoterate was introduced in 1989, gadoteridol in 1992, gadodiamide (Omniscan) in 1993, gadobutrol in 1998, and gadoversetamide (Optimark) in 1999. In addition to these CAs, gadobenate which was received by hepatocytes in the liver was released in 1998 and gadoxetic acid was introduced in 2005. CAs that contain gadofosveset and very small super-paramagnetic iron oxide (USPIO) particles can be used in MRA because they can remain in the vessel for a long time [54]. Gadolinium-based CAs are divided according to their ability to shorten relaxation time and their level of accumulation in tissue. Gadobutrol is the only gadolinium-based CA formulated as 1.0 m, which accumulates more in tissue and is twice the concentration of other agents. Due to its high relaxation, it is the maximum T1 shortening CA per volume [55–57].

When using the CA in MRA, the SNR increases, the flow and motion artifacts are reduced, because the paramagnetic Gd reduces the T1 relaxation time [58]. Evaluating the vessel lumen using the T1 sequence which is not affected by flow artifacts removes many problems in TOF or flow-based MR sequences. Turbulence decreases, resolution increases, high-speed MRA images with high SNR are obtained. If Gd is given at a high injection rate, the concentration increases, SNR increases, but if the concentration increases too much, it can reduce the signal with T2* effect. The T2* effects start if the injection is faster than 5 mL/s. It is necessary not to change the Gd concentration during the process because this may cause a ringing artifact. Also, if we make an injection with high speed for a long time, this causes too much Gd usage and high cost. It should also not exceed the FDA limit. For this reason, it would be correct to make an injection at a rate of 2–3 mL/s in less than the scan time to maximize the injection rate while keeping the dose minimum.

Although DSA is the gold standard in CS evaluation [59], it is an invasive method and noninvasive methods such as Doppler US, MRA, and CTA have come to the fore. Although there is no clear consensus about exactly what is the best option, MRA, CTA, and Doppler US is widely used in the diagnosis of CS. Since the 1990s, TOF MR has been used to detect CS with a specificity and sensitivity of more than 70% [60–62]. CE MRA can cover more of the carotid artery distribution in a fraction of time that TOF MRA is needed. Although there are plenty of papers, the optimal protocol for carotid CE MRA is still controversial.

Willinek et al. [63] compared CE MRA and DSA in the evaluation of lesions in supra-aortic arteries. They found the specificity, sensitivity, positive predictive value, and negative predictive value of CE MRA in detecting 70–90% stenosis was 99.3%, 100%, 93.6%, 100%, respectively. The same parameters were calculated as 100%, 100%, 100%, and 100% in the same order when evaluating the CE MRA occlusion. In this study, 0.2 mmol/kg Gd was used with an infusion rate of 3 mL/s, followed by 30 mL saline bolus. CE MRA, which is a noninvasive method in supra-aortic strictures, seems to be a good alternative to replace DSA.

Because of the complications such as nephrogenic systemic fibrosis which may develop after the use of CA, CAs should be used at the lowest dose or as low as possible. For this reason, methods such as TOF, which is an MRA protocol without CA become popular.

Fellner et al. [64] compared 3D TOF MRI with HR CE MRI and time-resolved CE MRA in the evaluation of carotid stenosis. When evaluating these three methods, they used DSA and endarterectomy specimens as the gold standard. The sensitivity of all MR methods in severe stenosis was 100%, while the specificity of 3D TOF MRI, HR CE MRI, and time-resolved CE MRA were 96.7%, 80.6%, and 83.9%, respectively. While 3D TOF MRI is better than others in grading stenosis at carotid bifurcation level, the best option should be to combine these methods. However, according to this study, TOF MRI seems to be adequate when evaluating the carotid arteries if the contrast administration is risky. If we evaluate how CA is used in contrast-enhanced MRA sequences in this study: In HR CE MRA, 25 mL of Gd-DTPA was given with a speed of 2 mL/s. Timing for the HR CE

sequence was performed with fluoroscopic triggering at one image/s. 3D MRA sequence was started manually when CA was seen in the common carotid arteries on the fluoroscopy. In time-resolved CE MRA four data sets were acquired consecutively, resulting in a timing interval of 10 s between successive data sets; no data sharing or temporal interpolation was employed. Instead of a dedicated timing procedure, measurement of the sequence and the injection of 15 mL of Gd-DTPA (2 mL/s) were started simultaneously. The data set showing the optimal arterial phase was selected afterward.

For the more widespread use of MRI in patients with stroke, the speed of MRI acquisition should be increased. In a study [65] conducted on the feasibility of low-dose CE MRA and dynamic contrast perfusion without extra CM, a total of 0.1 mmol/kg of Gd was given to patients (0.05 mmol/kg for CE MRA, 0.05 mmol/kg for dynamic contrast perfusion). This 0.1 mmol/kg CM was diluted with saline to a total of 50 mL. Transit time to the carotid artery was calculated with 3 mL of this 50 mL CM by flashing 20 mL of saline, and then 22 mL of contrast was flushed with 20 mL saline and CE MRA was performed. In this process, the contrast rate is set to 1.5 mL/s. The remaining 25 mL contrast was flushed with 20 mL saline and MR perfusion was performed. Here, the speed of contrast is set to 5 mL/s. In the full-dose group, the same procedure was performed without dilution. The half-dose CM group and full-dose CM group were compared with the DSA results and there was no significant difference between the two groups in terms of SNR, maximum T2 * effect, and detecting the degree of arterial stenosis.

In a study comparing 2D TOF MRA and CE MRA in patients with hemodynamically significant carotid stenosis [66], no significant difference was found between these two methods. In CE MRA, they gave 0.01 mmol/kg (or 0.2 mg/kg) CM as a single dose of 20 mL at a rate of 3 mL/s. Although CE MRA showed neurovascular structures better than 2D TOF MRA in this study, Gd administration did not provide any advantage in carotid stenosis requiring surgical treatment. Therefore, 2D TOF MRI may be sufficient to evaluate carotid stenosis patients with renal problems.

In a study [67], 3D HR MRA of supra-aortic arteries was performed with 3 T MRI scanner with three different contrast regimens, and patients were divided into three groups: high dose (group A), moderate dose (group B), and low dose (group C). Group A received 0.154 mmol/kg, group B received 0.097 mmol/kg, and group C received 0.047 mmol/kg Gd-DTPA. Incrementally, CA dose decreased from an initial dose of 12.5 mmol Gd-DTPA (0.5 mmol/mL in 25 mL) to 7.5 mmol and then to 3.875 mmol, based on clinical observation of the stability of image quality. In all dose levels, infusion time was fixed at 15 s, corresponding to 0.8 mmol/s for group A, 0.5 mmol/s for group B, and 0.25 mmol/s for group C. For the group B and C, CM was diluted with normal saline by factors of two and three, respectively, to maintain equivalent injected volumes and rates. According to the results of the study, it is possible to demonstrate the supra-aortic arteries at 3 T MRI with 3D CE MRA at a low CM dose of 0.047 mmol/kg without reducing the image quality.

Jung et al. [68] performed a study to determine the optimal dose of Gd-DTPA for CE MRA of intracranial vascular diseases. In this study, subjects suspected of having intracranial vascular diseases had cerebral MR angiograms on a 1.5 T unit. Patients were randomly assigned to receive one of four doses of Gd-DTPA (Magnevist; Schering, Berlin, Germany): 36 subjects received no injection, 37 received 5 mL (0.04 0.06 mmoVkg), 38 received 10 mL (0.08 0.12 mmoVkg), and 11 received 20 mL (0.15 0.25 mmol/kg). The other 30 subjects had unenhanced and CE MR angiography (10 subjects each for the 5 mI, 10 mI, and 20 mI groups). CE MR angiograms were obtained immediately after IV injection of a bolus of gadopentetate dimeglumine. 5–10 mL of Gd-DTPA appears to be sufficient for CE cerebral MR angiography. Injection of 20 mL of the CM frequently limited visualization of the major arteries because of venous overlap. 5–10 mL of Gd-DTPA appears to be an optimal dose range for CE cerebral MRA. Use of this dose can help in differentiating true stenosis of large arteries from artifactual narrowing and in

depicting small arteriovenous malformation with a slow flow.

TOF MRI is a very popular method since it does not require contrast and is used in the diagnosis of cerebral aneurysms. In a study [69], authors compared TOF MRA and CE MRA using the elliptical centric method with the 3 T MR scanner for the diagnosis of cerebral aneurysms. Using 2 mL of gadoteridol and 20 mL of saline flush, the time between injection and reaching of CM to the skull base level was calculated. 25 mL of gadoteridol followed by 25 mL of saline flush was given at 2 mL/s. In terms of image quality, TOF MRA was shown to be superior (Fig. 18.3).

In another similar study, 3D TOF MRA and CE MRA were used to evaluate cerebral aneurysms treated with flow diverter stents [70]. In the CE MRA process, 20 mL bolus CM followed by 30 mL saline flush was used. This time, CE MRA was found to be superior to TOF MRI in subjects such as the presence of residual filling in the aneurysm and parent artery patency (Fig. 18.4). If we look at how the contrast should be used in the MRA when grading cerebral AVMs [71], in 3 T MRI, with a two-cylinder injector, the Gd-DTPA in one cylinder and saline in the other cylinder is prepared then 20 mL Gd is given at 5 mL/s, followed by 40 mL of saline flush. With this protocol, in the CE MRA, the feeders, draining veins, and nidus of the AVM can be shown clearly.

There is a manganese-based alternative to Gd. Gale et al. [72] compared iv contrast enhancement produced by the manganese-based MRI CA manganese N picolyl N,N′,N′ trans 1,2 cyclohexenediaminetriacetate (Mn PyC3A) to Gd-DTPA and evaluated the excretion, pharmacokinetics, and metabolism of Mn PyC3A in baboons. Mn PyC3A was eliminated via renal and hepatobiliary excretion with similar pharmacokinetics to Gd-DTPA. High-performance liquid chromatography revealed no evidence of Mn PyC3A biotransformation. Mn PyC3A enables CE MRA with comparable contrast enhancement to Gd-based agents and may overcome concerns regarding Gd-associated toxicity and retention. Mn PyC3A may enable CE MRA in subjects with renal insufficiency who are currently contraindicated for Gd-based CAs.

New MR protocols and new CAs that are constantly evolving provide the opportunity to

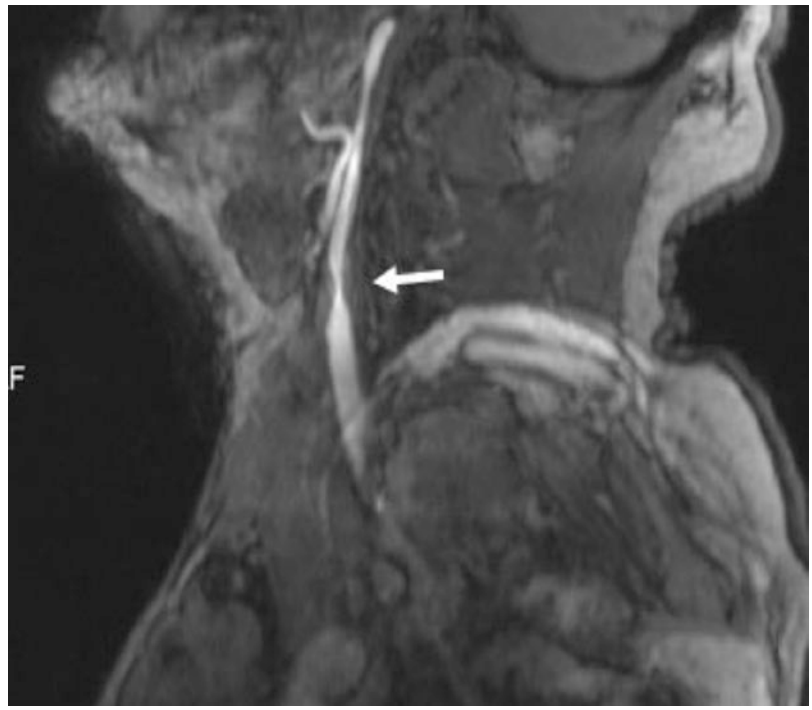

Fig. 18.3 2D TOF MRA showing stenosis in left ICA (arrow)

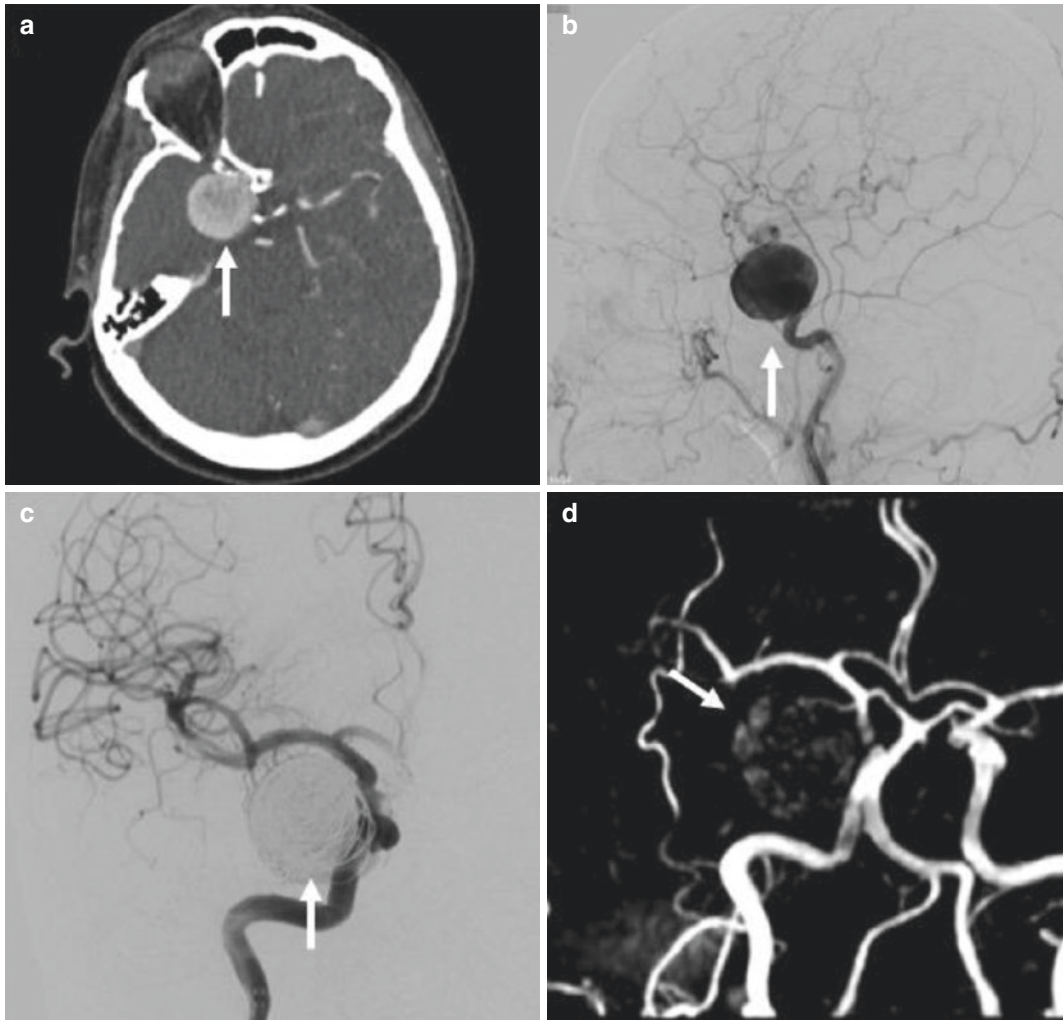

Fig. 18.4 CTA (**a**) and selective DSA of the right internal carotid artery (**b**) before treatment reveals a giant carotid ophthalmic aneurysm. DSA (**c**) and 2D TOF MRA (**d**) of the same aneurysm after coil embolization

receive radio anatomic or physiopathological additional information. It is extremely wrong to think that the positive acceleration progress in radiology especially in recent years has come to an end. We believe that new developments will cause a revision of some information in this section in the near future.

References

1. Orrison WW Jr, Snyder KV, Hopkins LN, et al. Whole-brain dynamic CT angiography and perfusion imaging. Clin Radiol. 2011;66(6):566–74.
2. Creasy JL, Price RR, Presbrey T, Goins D, Partain CL, Kessler RM. Gadolinium-enhanced MR angiography. Radiology. 1990;175(1):280–3.
3. Marchal G, Bosmans H, Van PH, Jiang YB, Aerts P, Bauer H. Experimental Gd-DTPA polylysine enhanced MR angiography: sequence optimization. J Comput Assist Tomogr. 1991;15(4):711–5.
4. Brenner DJ, Hricak H. Radiation exposure from medical imaging: time to regulate? JAMA. 2010;304(2):208–9.
5. Enterline DS, Kapoor G. A practical approach to CT angiography of the neck and brain. Tech Vasc Interv Radiol. 2006;9(4):192–204.
6. Koelemay MJ, Nederkoorn PJ, Reitsma JB, Majoie CB. Systematic review of computed tomographic angiography for assessment of carotid artery disease. Stroke. 2004;35(10):2306–12.

7. Schellinger PD, Fiebach JB, Hacke W. Imaging-based decision making in thrombolytic therapy for ischemic stroke: present status. Stroke. 2003;34(2):575–83.
8. Truwit CL. CT angiography versus MR angiography in the evaluation of acute neurovascular disease. Radiology. 2007;245(2):362–6.
9. Nederkoorn PJ, Mali WPTM, Eikelboom BC, et al. Preoperative diagnosis of carotid artery stenosis: accuracy of noninvasive testing. Stroke. 2002;33(8):2003–8.
10. Napel S, Marks MP, Rubin GD, et al. CT angiography with spiral CT and maximum intensity projection. Radiology. 1992;185(2):607–10.
11. Katz DA, Marks MP, Napel SA, Bracci PM, Roberts SL. Circle of Willis: evaluation with spiral CT angiography, MR angiography, and conventional angiography. Radiology. 1995;195(2):445–9.
12. Hollingworth W, Nathens AB, Kanne JP, et al. The diagnostic accuracy of computed tomography angiography for traumatic or atherosclerotic lesions of the carotid and vertebral arteries: a systematic review. Eur J Radiol. 2003;48(1):88–102.
13. Dillon EH, Van Leeuwen MS, Fernandez MA, Eikelboom BC, Mali WP. CT angiography: application to the evaluation of carotid artery stenosis. Radiology. 1993;189(1):211–9.
14. Cumming MJ, Morrow IM. Carotid artery stenosis: a prospective comparison of CT angiography and conventional angiography. AJR Am J Roentgenol. 1994;163(3):517–23.
15. Link J, Brossmann J, Grabener M, et al. Spiral CT angiography and selective digital subtraction angiography of internal carotid artery stenosis. Am J Neuroradiol. 1996;17(1):89–94.
16. Marcus CD, Ladam-Marcus VJ, Bigot JL, Clement C, Baehrel B, Menanteau BP. Carotid arterial stenosis: evaluation at CT angiography with the volume-rendering technique. Radiology. 1999;211(3):775–80.
17. Leclerc X, Godefroy O, Lucas C, et al. Internal carotid arterial stenosis: CT angiography with volume rendering. Radiology. 1999;210(3):673–82.
18. de Monyé C, Cademartiri F, de Weert TT, Siepman DA, Dippel DW, van Der Lugt A. Sixteen–detector row CT angiography of carotid arteries: comparison of different volumes of contrast material with and without a bolus chaser. Radiology. 2005;237(2):555–62.
19. Lell M, Wildberger JE, Heuschmid M, et al. CT-angiographie der A. carotis: erste erfahrungen mit einem 16-schicht-spiral-CT. In: RöFo-Fortschritte auf dem Gebiet der Röntgenstrahlen und der bildgebenden Verfahren 2002. Vol. 174, No. 09, p. 1165–69.
20. Ertl-Wagner B, Hoffmann RT, Brüning R, Dichgans M, Reiser MF. Supraaortale Gefäßdiagnostik mit dem 16-Zeilen-Multidetektor-Spiral-CT. Untersuchungsprotokoll und erste Erfahrungen. Radiologe. 2002;42(9):728–32.
21. Irie T, Kajitani M, Yamaguchi M, Itai Y. Contrast-enhanced CT with saline flush technique using two automated injectors: how much contrast medium does it save? J Comput Assist Tomogr. 2002;26(2):287–91.
22. Cademartiri F, van der Lugt A, Luccichenti G, Pavone P, Krestin GP. Parameters affecting bolus geometry in CTA: a review. J Comput Assist Tomogr. 2002;26(4):598–607.
23. Haage P, Schmitz-Rode T, Hübner D, Piroth W, Gunther RW. Reduction of contrast material dose and artifacts by a saline flush using a double power injector in helical CT of the thorax. Am J Roentgenol. 2000;174(4):1049–53.
24. Hopper KD, Mosher TJ, Kasales CJ, TenHave TR, Tully DA, Weaver JS. Thoracic spiral CT: delivery of contrast material pushed with injectable saline solution in a power injector. Radiology. 1997;205(1):269–71.
25. Cademartiri F, Mollet N, van der Lugt A, et al. Non-invasive 16-row multislice CT coronary angiography: usefulness of saline chaser. Eur Radiol. 2004;14(2):178–83.
26. Kim JJ, Dillon WP, Glastonbury CM, Provenzale JM, Wintermark M. Sixty-four-section multidetector CT angiography of carotid arteries: a systematic analysis of image quality and artifacts. Am J Neuroradiol. 2010;31(1):91–9.
27. Bae KT. Test-bolus versus bolus-tracking techniques for CT angiographic timing. Radiology. 2005;236(1):369.
28. Cademartiri F, Nieman K, van der Lugt A, et al. Intravenous contrast material administration at 16–detector row helical CT coronary angiography: test bolus versus bolus-tracking technique. Radiology. 2004;233(3):817–23.
29. Hallett RL, Fleischmann D. Tools of the trade for CTA: MDCT scanners and contrast medium injection protocols. Tech Vasc Interv Radiol. 2006;9(4):134–42.
30. Kayan M, Demirtas H, Türker Y, et al. Carotid and cerebral CT angiography using low volume of iodinated contrast material and low tube voltage. Diagn Interv Imaging. 2016;97(11):1173–9.
31. Cho ES, Chung TS, Oh DK, et al. Computed tomography angiography using a low tube voltage (80 kVp) and a moderate concentration of iodine contrast material: a quantitative and qualitative comparison with conventional computed tomography angiography. Invest Radiol. 2012;47(2):142–7.
32. Nagayama Y, Nakaura T, Tsuji A, et al. Cerebral bone subtraction CT angiography using 80 kVp and sinogram-affirmed iterative reconstruction: contrast medium and radiation dose reduction with improvement of image quality. Neuroradiology. 2017;59(2):127–34.
33. Zhao L, Li F, Zhang Z. Assessment of an advanced virtual monoenergetic reconstruction technique in cerebral and cervical angiography with third-generation dual-source CT: feasibility of using low-concentration contrast medium. Eur Radiol. 2018;28(10):4379–88.
34. Hinkmann FM, Voit HL, Anders K. Ultra-fast carotid CT-angiography: low versus standard volume contrast material protocol for a 128-slice CT-system. Invest Radiol. 2009;44(5):257–64.

35. Saba L, Sanfilippo R, Pirisi R, Pascalis L, Montisci R, Mallarini G. Multidetector-row CT angiography in the study of atherosclerotic carotid arteries. Neuroradiology. 2007;49(8):623–37.
36. Bae KT. Intravenous contrast medium administration and scan timing at CT: considerations and approaches. Radiology. 2010;256(1):32–61.
37. Bae KT, Heiken JP. Computer modeling approach to contrast medium administration and scan timing for multislice computed tomography. In: Multislice CT: a practical guide. Berlin, Heidelberg: Springer; 2001. p. 28–36.
38. Ruíz DSM, Murphy K, Gailloud P. 320-Multidetector row whole-head dynamic subtracted CT angiography and whole-brain CT perfusion before and after carotid artery stenting. Eur J Radiol. 2010;74(3):413–9.
39. Chang YM, Tsai AC, Gutierrez A. Effect of right-sided versus left-sided contrast injection on intra-arterial opacification characteristics of head and neck computed tomography angiograms and interactions with patient sex, weight, and cardiac output. J Comput Assist Tomogr. 2015;39(5):752–9.
40. Jo KI, Kim SR, Choi JH, Kim KH, Jeon P. Contrast-enhanced angiographic cone-beam computed tomography without pre-diluted contrast medium. Neuroradiology. 2015;57(11):1121–6.
41. Doerfler A, Engelhorn T, Von Kummer R. Are iodinated contrast agents detrimental in acute cerebral ischemia? An experimental study in rats. Radiology. 1998;206(1):211–7.
42. Rubin GD, Lane MJ, Bloch DA, Leung AN, Stark P. Optimization of thoracic spiral CT: effects of iodinated contrast medium concentration. Radiology. 1996;201(3):785–91.
43. Loubeyre P, Debard I, Nemoz C, Minh VAT. High opacification of hilar pulmonary vessels with a small amount of nonionic contrast medium for general thoracic CT: a prospective study. Am J Roentgenol. 2002;178(6):1377–81.
44. de Monyé C, de Weert TT, Zaalberg W, et al. Optimization of CT angiography of the carotid artery with a 16-MDCT scanner: craniocaudal scan direction reduces contrast material-related perivenous artifacts. Am J Roentgenol. 2006;186(6):1737–45.
45. Ross S, Spendlove D, Bolliger S, et al. Postmortem whole-body CT angiography: evaluation of two contrast media solutions. Am J Roentgenol. 2008;190(5):1380–9.
46. Moon M, Cornfeld D, Weinreb J. Dynamic contrast-enhanced breast MR imaging. Magn Reson Imaging Clin N Am. 2009;17(2):351–62.
47. Essig M, Dinkel J, Gutierrez JE. Use of contrast media in neuroimaging. Magn Reson Imaging Clin. 2012;20(4):633–48.
48. Yang S, Law M, Zagzag D, et al. Dynamic contrast-enhanced perfusion MR imaging measurements of endothelial permeability: differentiation between atypical and typical meningiomas. Am J Neuroradiol. 2003;24(8):1554–9.
49. Leiner T, Michaely H. Advances in contrast-enhanced MR angiography of the renal arteries. Magn Reson Imaging Clin N Am. 2008;16(4):561–72.
50. Keston P, Murray AD, Jackson A. Cerebral perfusion imaging using contrast-enhanced MRI. Clin Radiol. 2003;58(7):505–13.
51. Lima JA. Myocardial viability assessment by contrast-enhanced magnetic resonance imaging. J Am Coll Cardiol. 2003;42(5):902–4.
52. Catalano OA, Manfredi R, Vanzulli A, et al. MR arthrography of the glenohumeral joint: modified posterior approach without imaging guidance. Radiology. 2007;242(2):550–4.
53. Lohrke J, Frenzel T, Endrikat J, et al. 25 years of contrast-enhanced MRI: developments, current challenges and future perspectives. Adv Ther. 2016;33(1):1–28.
54. Bremerich J, Bilecen D, Reimer P. MR angiography with blood pool contrast agents. Eur Radiol. 2007;17(12):3017.
55. Sieber MA. Pharmaceutical and safety aspects of gadolinium-based contrast agents. 2009;15(6):24–6.
56. Rohrer M, Bauer H, Mintorovitch J, Requardt M, Weinmann HJ. Comparison of magnetic properties of MRI contrast media solutions at different magnetic field strengths. Invest Radiol. 2005;40(11):715–24.
57. Cheng KT, Cheng HY, Leung K. Clinical use of gadobutrol for contrast-enhanced magnetic resonance imaging of neurological diseases. Rep Med Imaging. 2012;5:15–22.
58. Zhang H, Maki JH, Prince MR. 3D contrast-enhanced MR angiography. J Magn Reson Imaging. 2007;25(1):13–25.
59. DeMarco JK, Huston J, Nash AK. Extracranial carotid MR imaging at 3T. Magn Reson Imaging Clin. 2006;14(1):109–21.
60. Anderson CM, Lee RE, Levin DL, De la Torre Alonso S, Saloner D. Measurement of internal carotid artery stenosis from source MR angiograms. Radiology. 1994;193(1):219–26.
61. Kent KC, Kuntz KM, Patel MR, et al. Perioperative imaging strategies for carotid endarterectomy: an analysis of morbidity and cost-effectiveness in symptomatic patients. JAMA. 1995;274(11):888–93.
62. Patel MR, Kuntz KM, Klufas RA, et al. Preoperative assessment of the carotid bifurcation: can magnetic resonance angiography and duplex ultrasonography replace contrast arteriography? Stroke. 1995;26(10):1753–8.
63. Willinek WA, von Falkenhausen M, Born M, et al. Noninvasive detection of steno-occlusive disease of the supra-aortic arteries with three-dimensional contrast-enhanced magnetic resonance angiography: a prospective, intra-individual comparative analysis with digital subtraction angiography. Stroke. 2005;36(1):38–43.
64. Fellner C, Lang W, Janka R, et al. Magnetic resonance angiography of the carotid arteries using three different techniques: accuracy compared with intraarterial

x-ray angiography and endarterectomy specimens. J Magn Reson Imaging. 2005;21(4):424–31.
65. Nael K, Meshksar A, Ellingson B, et al. Combined low-dose contrast-enhanced MR angiography and perfusion for acute ischemic stroke at 3T: a more efficient stroke protocol. Am J Neuroradiol. 2014;35(6):1078–84.
66. Babiarz LS, Romero JM, Murphy EK, et al. Contrast-enhanced MR angiography is not more accurate than unenhanced 2D time-of-flight MR angiography for determining ≥ 70% internal carotid artery stenosis. Am J Neuroradiol. 2009;30(4):761–8.
67. Tomasian A, Salamon N, Lohan DG, Jalili M, Villablanca JP, Finn JP. Supraaortic arteries: contrast material dose reduction at 3.0-T high-spatial-resolution MR angiography—feasibility study. Radiology. 2008;249(3):980–90.
68. Jung HW, Chang KH, Choi DS, Han MH, Han MC. Contrast-enhanced MR angiography for the diagnosis of intracranial vascular disease: optimal dose of gadopentetate dimeglumine. AJR Am J Roentgenol. 1995;165(5):1251–5.
69. Gibbs GF, Huston J III, Bernstein MA, Riederer SJ, Brown RD Jr. 3.0-Tesla MR angiography of intracranial aneurysms: comparison of time-of-flight and contrast-enhanced techniques. J Magn Reson Imaging. 2005;21(2):97–102.
70. Attali J, Benaissa A, Soize S, Kadziolka K, Portefaix C, Pierot L. Follow-up of intracranial aneurysms treated by flow diverter: comparison of three-dimensional time-of-flight MR angiography (3D-TOF-MRA) and contrast-enhanced MR angiography (CE-MRA) sequences with digital subtraction angiography as the gold standard. J Neurointerv Surg. 2016;8(1):81–6.
71. Oleaga L, Dalal SS, Weigele JB, et al. The role of time-resolved 3D contrast-enhanced MR angiography in the assessment and grading of cerebral arteriovenous malformations. Eur J Radiol. 2010;74(3):e117–21.
72. Gale EM, Wey HY, Ramsay I, Yen YF, Sosnovik DE, Caravan P. A manganese-based alternative to gadolinium: contrast-enhanced MR angiography, excretion, pharmacokinetics, and metabolism. Radiology. 2017;286(3):865–72.